K&C Science Report – Phase 1
Forestry Theme – Boreal Forest Mapping in Siberia

Christian Thiel
Friedrich-Schiller-University Jena, Loebdergraben 32, Christian.Thiel@uni-jena.de

Christiane Schmullius
Friedrich-Schiller-University Jena, Loebdergraben 32, c.schmullius@uni-jena.de

Maurizio Santoro
Gamma Remote Sensing, santoro@gamma-rs.ch

***Abstract*—This report provides on overview on the accomplished work done by the Friedrich-Schiller-University in the framework of the K&C initiative. Major aim was the derivation of forestry related thematic information over the whole prototype area which is located in Central Siberia. First of all a sophisticated SAR data processing chain had to be developed to handle the large amount of data. Afterwards four diverse classification strategies have been developed. These strategies comprise multitemporal methodologies, change detection and the implementation of interferometric coherence. In particular the latter strategy proved being valuable and having the potential for operational implementation.**

***Index Terms*—ALOS PALSAR, K&C Initiative, Forest Theme, Forest Cover Mapping, Change Mapping, Coherence, Siberia**

1. INTRODUCTION

SAR DATA offer great potential for forest cover mapping, forest disturbance mapping (e.g. logging, forest fire, and wind damage) and forest biomass assessment. Lower radar frequencies turned out to be of particular adequacy. E.g. L-band SAR backscatter data acquired by the JERS-1 SAR was found to be suitable for mapping forest cover in the boreal zone. Radar backscatter and interferometric coherence have been successfully implemented. The launch of ALOS PALSAR offers new dimensions regarding spaceborne SAR data driven investigations. Compared to its antecessor JERS-1, PALSAR features a much increased performance in terms of image radiometry, geometry, and orbit steadiness. The controlled interferometric baseline combined with the well-defined observation strategy over the boreal zone greatly increases the potential of interferometry based SAR data examinations.

The report first investigates the use of backscattered intensity and then evaluates the additional information obtained through synergistic use of intensity and coherence for large area forest monitoring in Siberia. Regarding the intensity a multitemporal approach and a change detection method have been developed. These mapping exercises are conducted on a pixel level. The mapping by means of intensity and coherence is based on image segments.

2. SAR DATA PROCESSING

A. SAR DATA PRE-PROCESSING

The SAR pre-processing comprehends the processing steps summarised in Figure 1. Unfortunately, still (also at cycle 20) partially erroneous data (intensity ramps) were delivered. These intensity ramps at the edges of the data stripes could appear at far and near range as well at both azimuth sides. The magnitude and the width of the erroneous parts were varying. For sustaining as many rows and lines as possible, an interactive approach was chosen instead of a fixed cutting scheme (compare Figure 2).

The DEM based (SRTM, 90 m) orthorectification is described by Wegmüller 1999. Each strip was processed separately; one lookup table was applied to both polarisations. Regarding topographic normalisation pixel area correction and angular adjustment as proposed by Castel at al. 2001 was implemented:

$$A_{slope} = \frac{az \cdot r}{\cos(\psi)} \qquad (1)$$

where *az* and *r* denote azimuth and range pixel spacing respectively, and ψ represents the projection angle, which is defined as angle between surface normal and image plane normal. The true local SAR pixel size A_{slope} is then used to correct for topography induced pixel area distortions as follows:

$$\sigma^0{}_{cor} = \sigma^0 * \frac{A_{flat}}{A_{slope}} \qquad (2)$$

where A_{flat} is the SAR pixel size for flat terrain, σ^0 is the backscattering coefficient, and $\sigma^0{}_{cor}$ the corrected backscattering coefficient. The angular adjustment utilises the incidence angle θ_{ref} for flat terrain and the actual local incidence angle θ_{loc} to minimise variations in backscatter which are caused by topography driven variations of backscattering mechanisms.

$$\sigma^0{}_f = \sigma^0{}_{\theta_{cor}} \left(\frac{\cos\theta_{ref}}{\cos\theta_{loc}} \right)^n \tag{3}$$

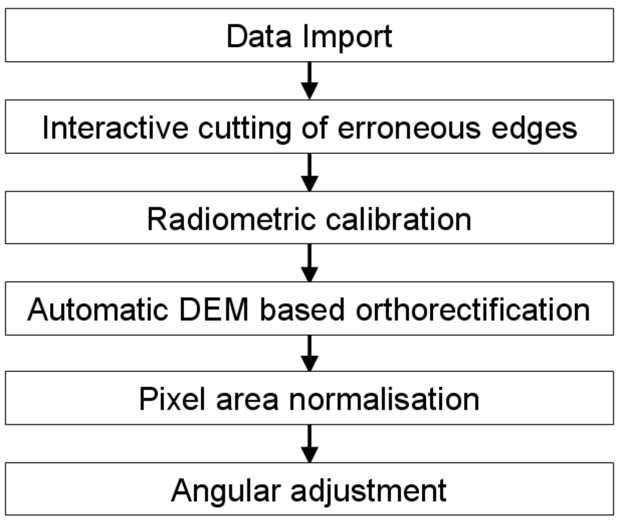

Figure 1: Scheme of K&C SAR data strip pre-processing

The geocoding accuracy was not checked in detail but can be assumed being high. The RMS errors between the automatically detected GCPs and the computed polynomials are in the order of 0.3 pixels. Geocoding details are preserved for each single strip and can be delivered if required. Figure 2 demonstrates this high geolocation precision. The black vertical fissure is due to missing data between the two strips. At the position were both data strips connect no geolocation offset is detectable. Additionally, no offsets have been detected during the multitemporal data examinations.

B. MOSAICING PROCEDURE

Mosaicing was conducted after SAR data pre-processing. Four mosaics, one for each cycle (08, 12, 13, and 20), have been processed. Areas with no data have been masked out. Histogram adaptation or similar radiometric adjustments have not been utilised. In the overlap area between two stripes feathering was applied with a maximum of 50 pixels (50 pixels when the data overlap was at least 50 pixels). Eventually, the mosaics from the cycles 12, 13, and 20 have been combined to one single multitemporal mosaic to achieve the maximised spatial coverage for prototype area-wide landcover classification. The intensities are scaled in dB.

C. FINAL DATA SETS

Figure 3 and Figure 4 provide an overview on the processed data for the K&C prototype area. Data has been processed up to ~62°N, while the prototype area extends to 65°N. However, due to geocoding problems (only minor relief north of 62°N and no adequate DEM available) it was considered to exclude the northern part of the prototype area for the time being.

None of the cycles provides a complete spatial coverage. Thus, multitemporal classification is not feasible for the whole prototype area. The lowest coverage was achieved for cycle 8. By means of combining all summer acquisitions an almost complete coverage of the prototype area can be achieved (see section 3.B).

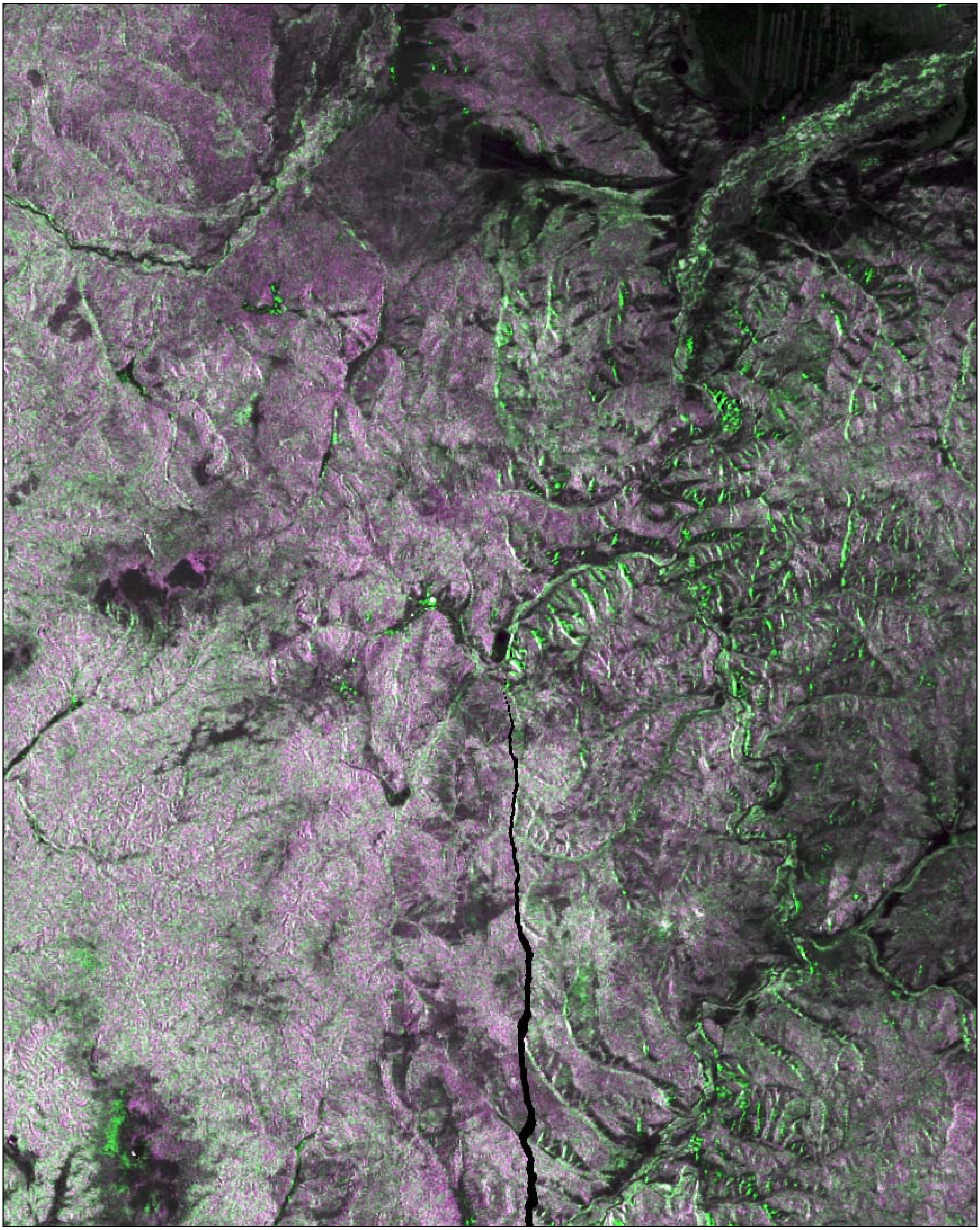

Figure 2: PALSAR HV/HH/HV composite for demonstration of high geolocation precision, ALOS K&C © JAXA/METI

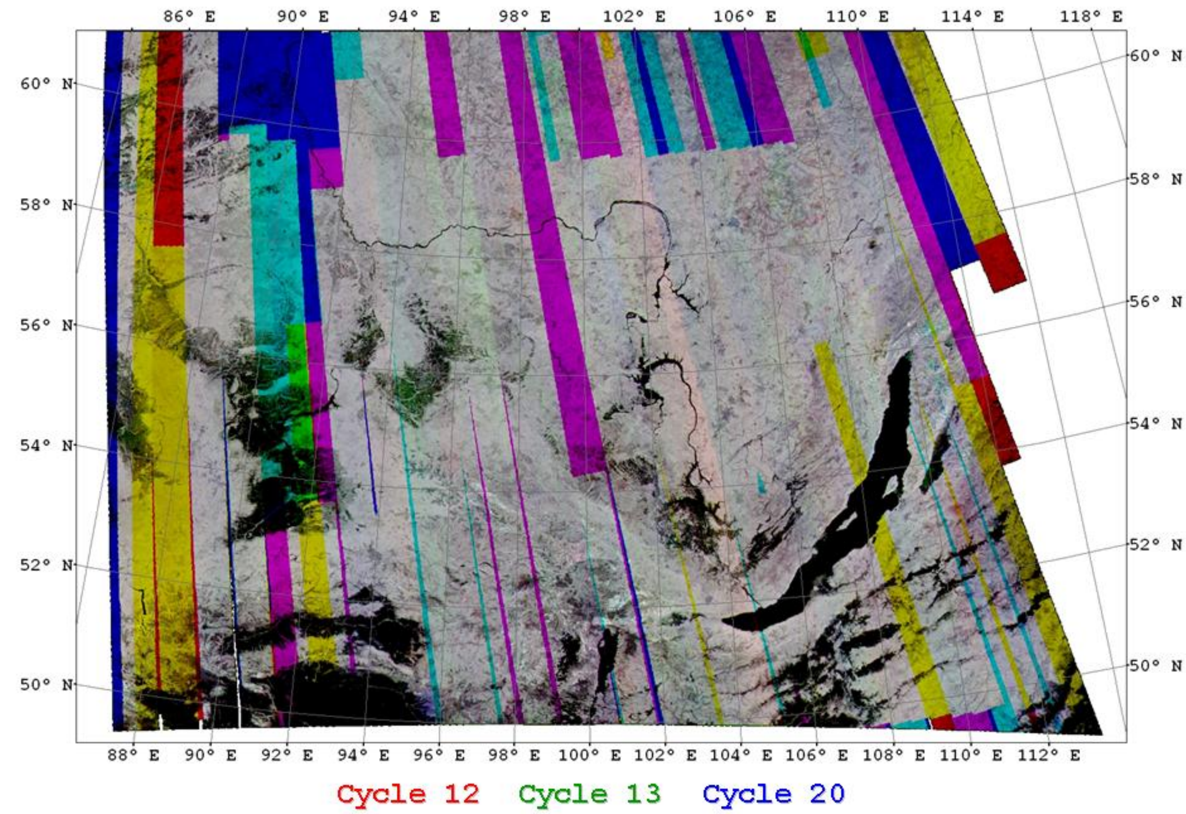

Figure 3: Processed summer FBD data in Siberia, ALOS K&C © JAXA/METI

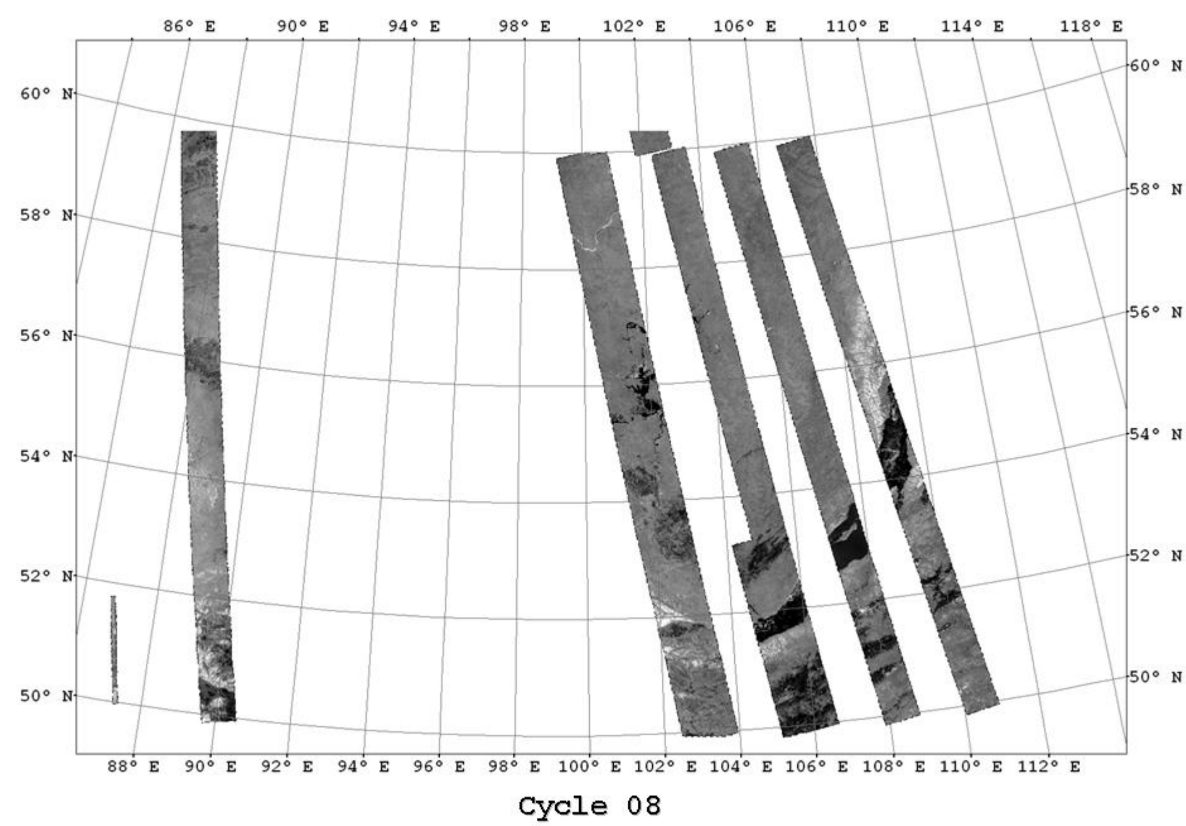

Figure 4: Processed winter FBS data in Siberia, ALOS K&C © JAXA/METI

3. CLASSIFICATION

A. *MULTITEMPORAL CLASSIFICATION*

CLASSIFICATION METHODOLOGY

The multitemporal classification makes use of the characteristic temporal backscattering variations of the considered classes. Thus, additionally to the multitemporal dataset, simple multitemporal metrics have been computed. The following table summarises the utilised data layers. The multitemporal metrics have been computed for both polarisations separately.

Basing on these preconditions suited and robust metrics have been selected and thresholds for the considered classes have been defined. These thresholds are summarised in the following table. All conditions per line in the table must be fulfilled. The classes water and settlement are defined manifold. In these cases at least on of the definitions must be fulfilled. However, at some positions within the test area higher backscatter values occur at water bodies. This is due to an uneven water surface caused by wind or currents (in particular at river junctions). To overcome the wind problem the minimum backscatter for HH was chosen. However, the current problem could not be completely solved in doing so.

PALSAR Data	Multitemporal Metrics
FBD HH/HV Cycle 12 (early summer 2007) FBD HH/HV Cycle 13 (late summer 2007) FBD HH/HV Cycle 20 (early summer 2008)	Minimum Mean Maximum Standard Deviation (averaged by 5x5 matrix)

Aim of the multitemporal classification was to separate as many land cover types as possible. The classification considers the land cover types water, agriculture, settlement, clear-cuts & burnt areas, three forest classes, and a class containing recent changes such as new clear-cuts (formed between cycles 12 and 20) and fire scars. The following table collects typical relative values for the available data layers from very high (++) to very low (--), 0 means medium values. These ratings are basing on fundamental knowledge and the examination of the available data.

Potential misclassifications concern agricultural fields featuring a smooth surface and low temporal variations. Forests are characterised by very stable backscatter. In comparison to other land cover types the backscattering intensity is high, in particular at cross polarisation. The amount of backscatter is a function of forest biomass, whereby saturation occurs already at rather low biomass levels. Nevertheless three forest classes have been established against different backscattering levels. Forest 1 is forest with no evidence (related to PALSAR data) for disturbances, forest 2

	HH Min	HH Mean	HH Max	HH Std.	HV Min	HV Mean	HV Max	HV Std.
Water	--	-	0	-	--	--	-	0
Agriculture	--	--	0	++	--	-	0	0
Forest 1 (dense, high biomass)	+	+	+	--	++	++	++	--
Forest 2 (low biomass)	0	0	0	--	0	0	0	--
Forest 3 (very low biomass)	-	-	-	-	-	-	-	-
Clear-cuts & burnt areas	--	-	-	-	--	--	-	-
Settlement	++	++	++	+	0	+	+	+
New clear-cuts and fire scars	--	0	+	++	--	0	++	++

	HH Min	HH Mean	HH Max	HH Std.	HV Min	HV Mean	HV Max	HV Std.
Water (Def. 1)	< -19 dB					< -26 dB		
Water (Def. 2)	< -16 dB			< 1.0		< -26 dB		
Water (Def. 3)	< -19 dB				< -30 dB			
Forest 1 (dense, high biomass)		< -2 dB					> -14 dB	< 1.2
Forest 2 (low biomass)		< -2 dB					> -17 dB	< 1.0
Forest 3 (very low biomass)		< -2 dB					> -20 dB	< 0.8
Settlement (Def. 1)		> -1 dB	> 0 dB	> 1.0				
Settlement (Def. 2)		> -3 dB	> -2 dB	> 2.0				
New clear-cuts and fire scars		< -4 dB				> -18 dB	> -14 dB	> 1.2
Clear-cuts & burnt areas		> -9 dB		< 2.0				
Agriculture		< -9 dB		> 2.0				

corresponds to former clear-cuts or fire scars with considerable regrowth and forest 3 is related to initial regrowth or other temporally stable forestry related classes with low to medium cross polarisation backscatter.

Settlements typically feature very high HH backscattering intensities. This particularly applies if geometric features of the settlements allow the generation of double bounce. Although settlements and their entities are rather stable in time, the backscattering intensity varies considerably. On the one hand, very high backscatter causes a high potential for very high variations, on the other hand, the amount of double bounce is driven by a number of variable conditions such as surface moisture or local incidence angle. In summary, only the parts of the settlements causing double bounce are detected as settlements. The other parts do not feature settlement specific backscattering signatures. Texture was not considered, as 50 m ground resolution cannot resolve relevant settlement objects.

New clear-cuts and fire scars must feature forest typical backscattering signatures at least at one (the first) acquisition date, thus maximum backscatter must be the same as for forest. The conversion from forest to non-forested areas causes high backscatter variations.

The remaining and so far not classified areas are agricultural land and clear-cuts / burnt areas with a maximum HV backscatter below -20 dB (minor volume scattering). This mixture can be segregated by the fact, that agricultural land is characterised by high temporal changes and thus high backscatter variations. Additionally, the mean HH backscatter is much lower compared to clear-cuts and burnt areas in particular. Although this multitemporal classification approach shows promising results (see below), the dataset in terms of the multitemporal dimension is not sufficient. For the derivation of multitemporal metrics with statistical significance many more acquisitions would have been required. The accuracy of all classes would benefit from such an extension of the data set. Still it could be demonstrated, that in principle an operational classification approach basing on multitemporal PALSAR data is feasible.

TEST AREA AND RESULTS

As a multitemporal dataset is required, the classification approach could not be applied to the whole prototype area. Thus, a spatial subset was created. The area covered by the tracks 467 and 468 of cycle 08 was taken as subset from 54°N to 60°N (see Figure 5). For this area data from all cycles (8, 12, 13, and 20) were available. Unfortunately, as emerged during the classification process, a single winter intensity scene (cycle 08) does not add supplementary information. Thus, data from cycle 08 was neglected.

Figure 5 provides an RGB composite of the whole subset and the final map. Figure 6 provides the same information for a part of the subset. Accuracy assessment has not been accomplished so far. However, at first view the classification results seem to be promising. The greatest potential for misclassifications lies in the fuzziness of the classes related to diverse biomasses. Thus, the classes forest 3 and clear-cuts & burnt areas contain thematically similar land cover types and could be merged later on. Also, the subdivision of the three forest classes was conducted arbitrarily. No scientific, political or economical definition of the class forest was considered. The class settlement is obviously heavily underestimated.

B. CLASSIFICATION OF BASIC LANDCOVER FOR WHOLE PROTOTYPE AREA

CLASSIFICATION METHODOLOGY

Mapping was conducted by means of thresholds using one single mosaic (FBD intensities) for the whole prototype area. This mosaic contains data from three different observation cycles; the focus was put on filling data gaps. As none of the cycles is delivered completely, the mosaic contains data from two different years. This approach can provide a map with the most complete coverage of the prototype area but with the lowest accuracy.

Figure 7 (top) shows a composite of the complete mosaic. As no histogram adaptation was conducted during the mosaicing process, some of the strips do not fit into the mosaic regarding their radiometry. This is most likely due to varying weather condition at the diverse acquisitions. Moreover, it can be observed, that the radiometric difference between two adjacent strips is varying, which complicates histogram matching efforts.

Aim of the multitemporal classification was to separate only basic land cover types. The classification considers the land cover types water, forest/settlement, and very low biomass (agriculture, clear-cuts, fire scars, steppe etc.). The following table collects typical mean relative values for the available data layers from very high (++) to very low (--), 0 means medium values. These ratings are basing on basic knowledge and examination of the available data.

	HH	HV
Water	--	--
Forest/Settlements	+	++
Very low biomass	-	-

As relatively broad classes have been considered, the signature spectrum of these classes exhibit great potential for overlaps. This is particularly true for the classes water and very low biomass. However, as no multitemporal metrics can be computed, the separation of more classes is not feasible. The table below summarised the thresholds for the classification. All conditions per line in the table must be fulfilled.

	HH	HV
Water	< -19 dB	< -26 dB
Forest/Settlements	> -8 dB	> -20 dB
Very low biomass	Remaining values	Remaining values

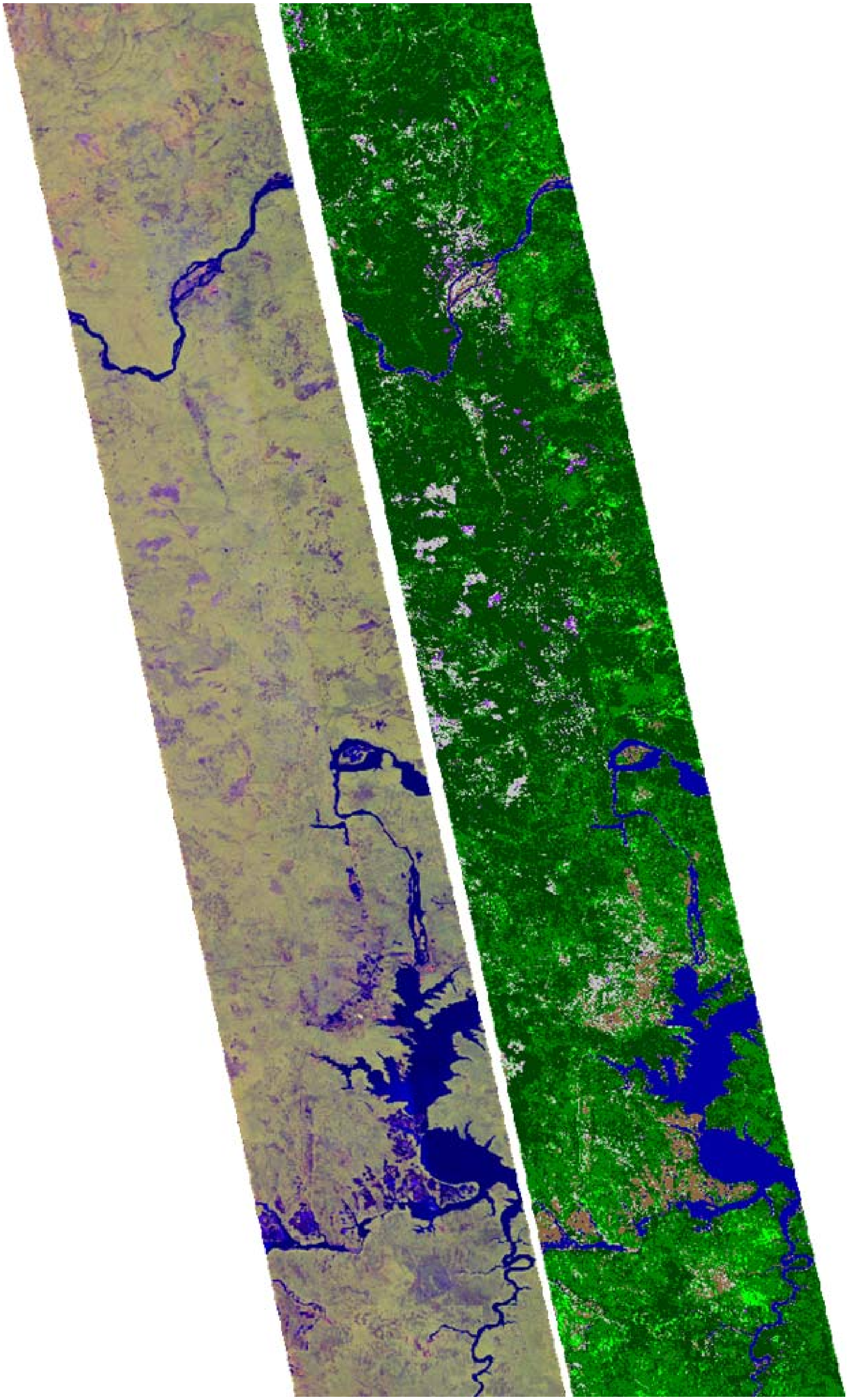

Figure 5: SAR data (left) and classification result (right) for the whole subset. SAR data composite and map colour coding as at Figure 6. (Tracks 467 and 468, 54°N-60°N), ALOS K&C © JAXA/METI

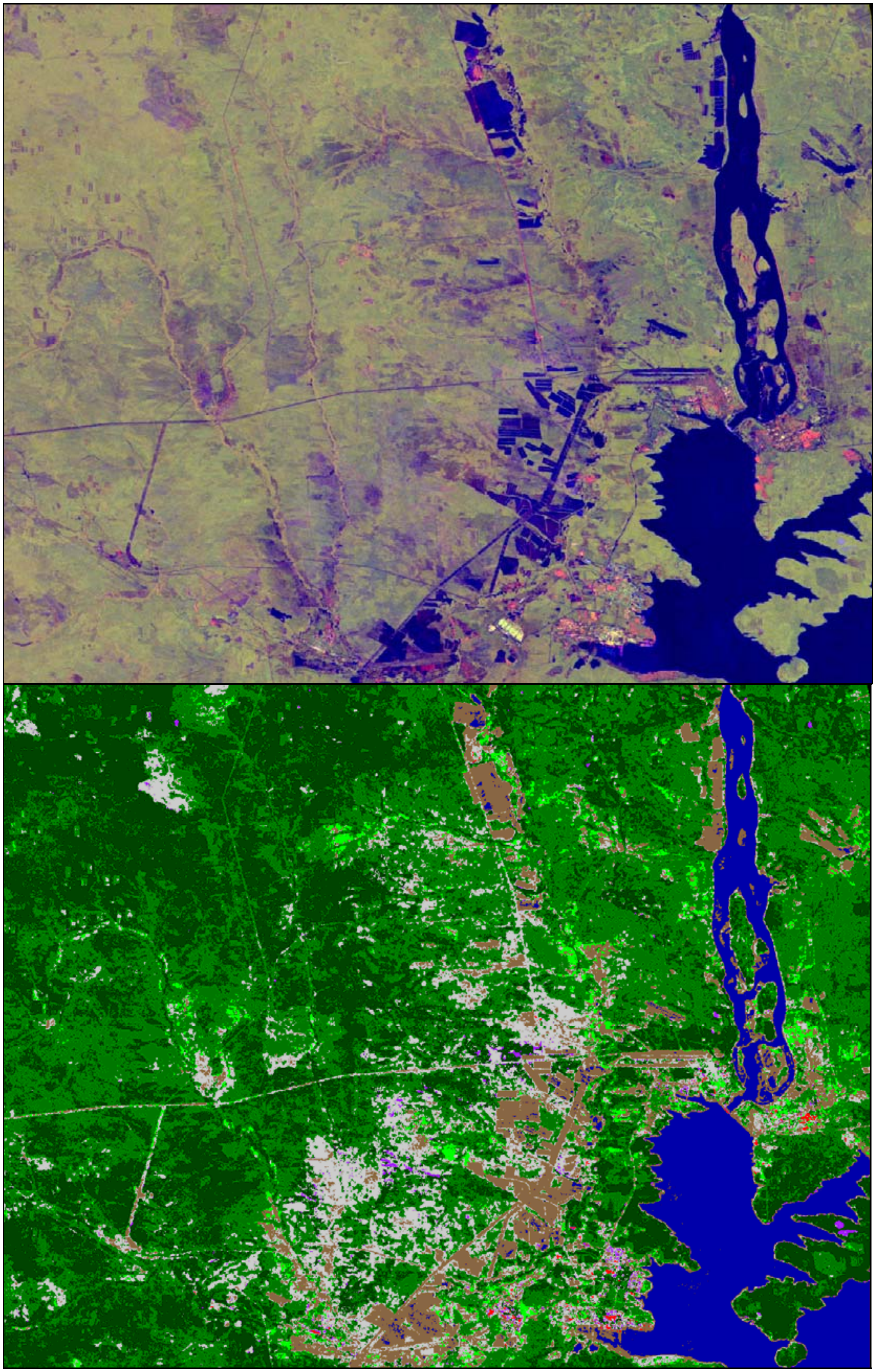

Figure 6: SAR data (top) and classification result (bottom) for part of subset. SAR data composite: HH mean / HV mean / HV std. dev.; Colour coding map: water (blue), forest dense (dark green), forest low biomass (green), forest very low biomass (light green), settlement (red), agriculture (brown), clear-cuts & burnt areas (grey), new clear-cuts and fire scars (purple), ALOS K&C © JAXA/METI

TEST AREA AND RESULTS

The result of the basic landcover classification for the whole prototype area is provided by Figure 7 (bottom) for the complete area and by Figure 8 for a subset of the area. The subset covers the same area as the map provided by Figure 6. Even if no accuracy assessment has been conducted so far it is obvious, that misclassifications are occurring. In particular the separation of water and very low biomass areas is not satisfying at all. In particular the steppe area in Tuwa (south-western edge of the area) produces very low backscatter and cannot be separated from water. A similar problem can also be observed at the subset of this map (Figure 8, compare with Figure 6). Very low biomass areas are in general well detected, however further separation of this mixes class is not feasible. Also at this subset significant confusion between water and very low biomass is obvious. Multitemporal data (important for agricultural areas) or even better coherence data would overcome this separation problem.

C. CLASSIFICATION OF CHANGES

CLASSIFICATION METHODOLOGY

Aim of the classification of changes is to detect areas with short term changes in land cover. Changes refer to deviation in land cover between cycle 12 and cycle 20. Due to radiometric deviations between the stripes the changes have to be detected stripe-wise. The classification of changes was not conducted for the whole prototype area, but for a subset. The subset is defined by the data coverage of track 468.

Input for the classification was the normalised backscatter difference index *NDBI*. This change measure was derived as follows:

$$NBDI_{XX} = \left\langle \frac{\sigma^0{}_{XX\,f_{t1}} - \sigma^0{}_{XX\,f_{t2}}}{\sigma^0{}_{XX\,f_{t1}} + \sigma^0{}_{XX\,f_{t2}}} \right\rangle \tag{4}$$

The *NBDI* is computed for each polarisation separately. The indices *t1* and *t2* denote the two different acquisitions. The idea of normalising the backscatter difference was to achieve a better comparability between the different tracks and to reduce the impact of different weather conditions. No change and equal radiometric properties of both strips result in an *NBDI* of zero. Negative values flag areas with a decrease in backscatter and vice versa. Potential changes in the investigated area are related to agricultural activities and forest management. New fire scars and in particular clear-cuts will cause a reduction of backscatter and thus negative *NBDI* values. Forest regrowth could result in increasing backscatter. However, only minor effects can be expected. Major source of positive *NBDI* values are agricultural areas with respective crop rotations.

Basing on the *NBDI* thresholds have been defined. These thresholds are summarised in the following table. All conditions per line in the table must be fulfilled. The class significant decrease of backscatter is defined twofold. At least on of the definitions must be fulfilled. The considered classes do not allow a statement on the actual change regarding the land cover type. These classes can be interpreted as change indicators. However, the combination of the change classification with the information derived by means of the multitemporal classification can close this gap.

	$NBDI_{HH}$	$NBDI_{HV}$
Significant increase of backscatter	0.25	0.10
Significant decrease of backscatter	-0.04	-0.02
Significant decrease of backscatter	-0.15	

TEST AREA AND RESULTS

Input data and results for the change classification are presented in following. Figure 9 depicts the input data represented as *NBDI* RG (red-green) colour composite, where red represents the *NBDI* for HH and green for HV. Thus, bright areas flag areas with increasing backscatter, dark areas vice versa. Different hues are caused be unequal change of backscatter regarding the two polarisations. The change map is provided by Figure 10. Although only one year passed by between the two acquisitions, much change is visible. However, most of the change is due to agricultural activities. Such areas can be recognised by a heterogeneous pattern of increasing and decreasing backscattering intensity (as e.g. in the middle of the fourth tile of track 468).

Figure 11 provides two subsets of the above presented dataset. The upper image pair represents a forest dominated area, the lower pair an agricultural area. The clear-cuts in the forest dominated section are obviously well captured by the change map. The massive change signal at the lower pair is most likely caused by crop rotation effects. Although the change map product is not yet validated, it seems to be a promising indicator for forestry related changes. Major issue is to separate the impacts of agriculture and clear-cutting (and forest fires). One solution could be the implementation of the multitemporal classification (section A).

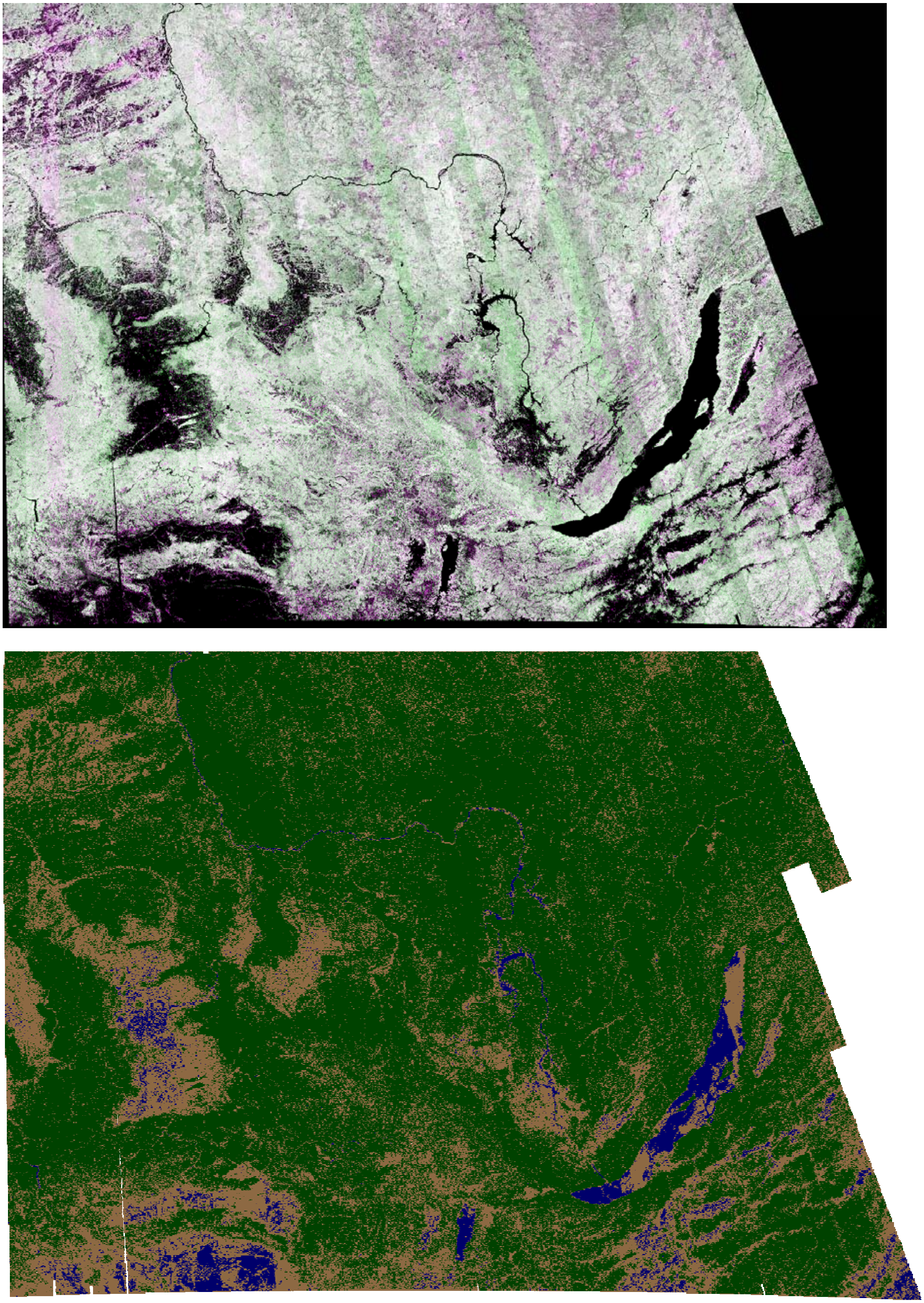

Figure 7: SAR data (top) and classification result (bottom) of prototype area. SAR data composite: HH/HV/HH; Colour coding map: water (blue), forest/settlements (dark green), very forest low biomass (brown) , ALOS K&C © JAXA/METI

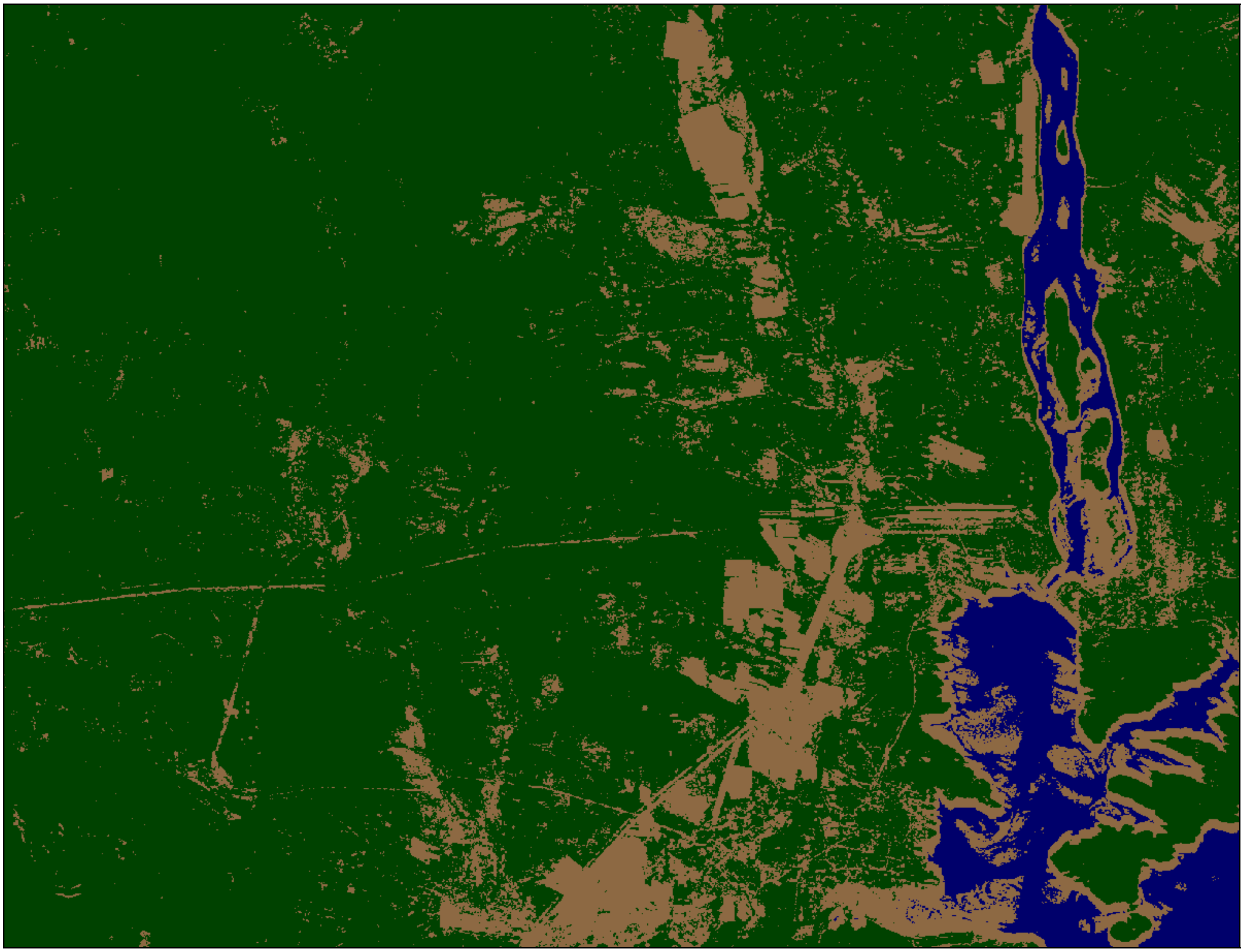

Figure 8: Classification result for subset of prototype area. Colour coding map: water (blue), forest/settlements (dark green), very forest low biomass (brown) , ALOS K&C © JAXA/METI

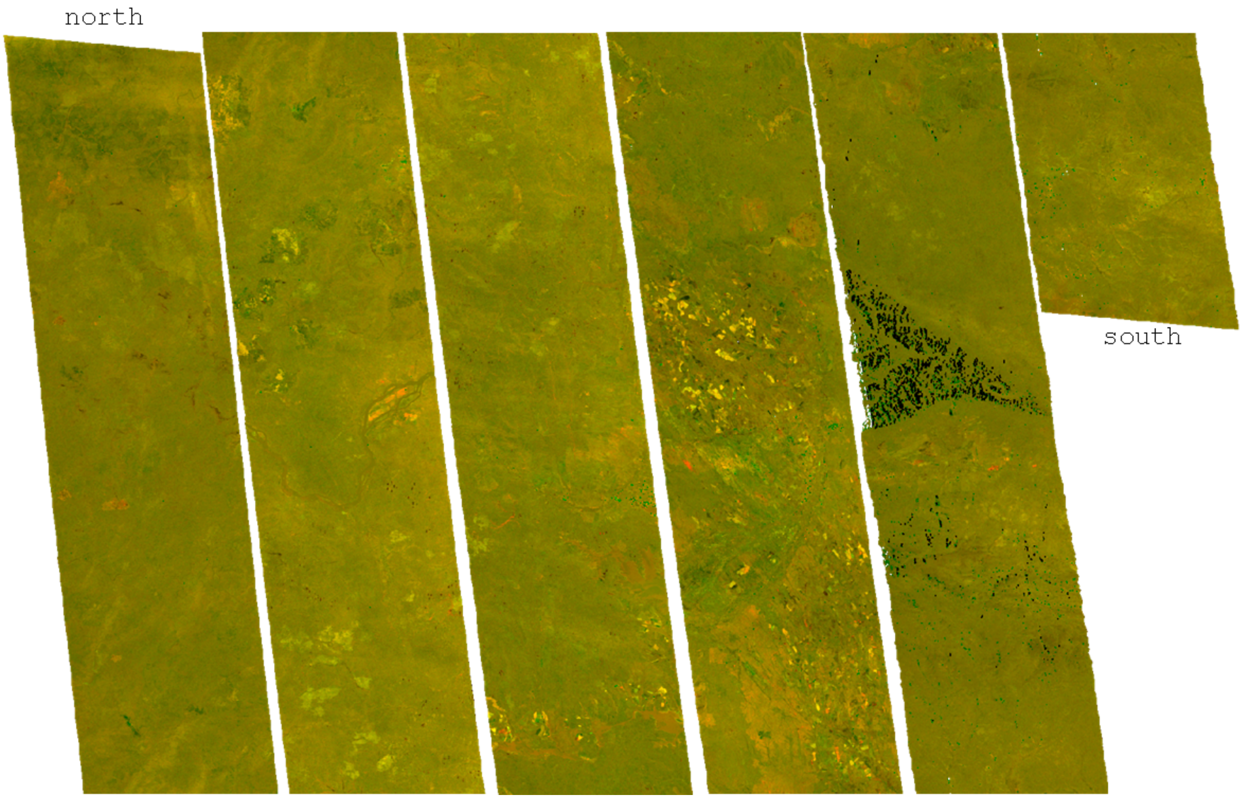

Figure 9: Input data for change map generation: Normalised Backscattering Difference Index (NBDI) of cycles 12 and 20 (RG composite: HH NBDI /HV NBDI). Data taken from track 468, fragmented for better overview, ALOS K&C © JAXA/METI

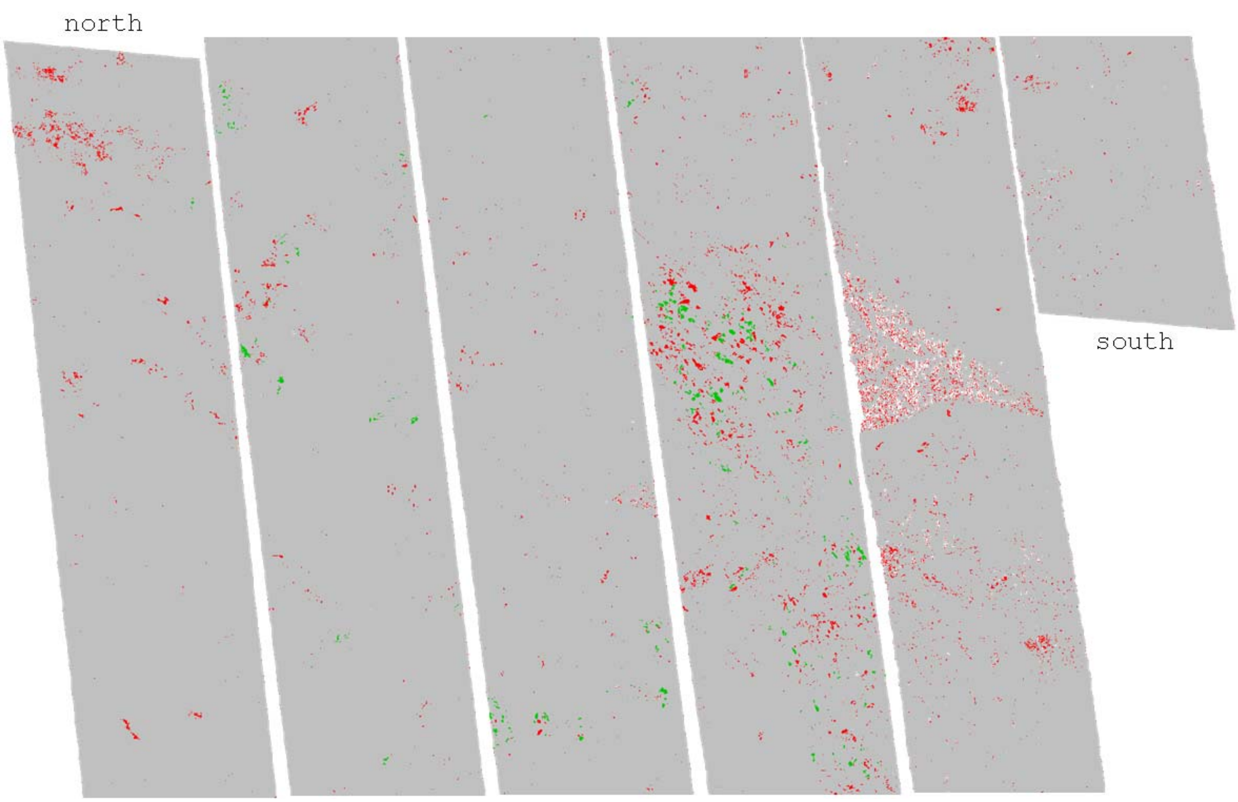

Figure 10: Change map. Colour coding: grey: no change, white: no data, red: decrease of backscatter, green: increase of backscatter. Data taken from track 468, fragmented for better overview, ALOS K&C © JAXA/METI

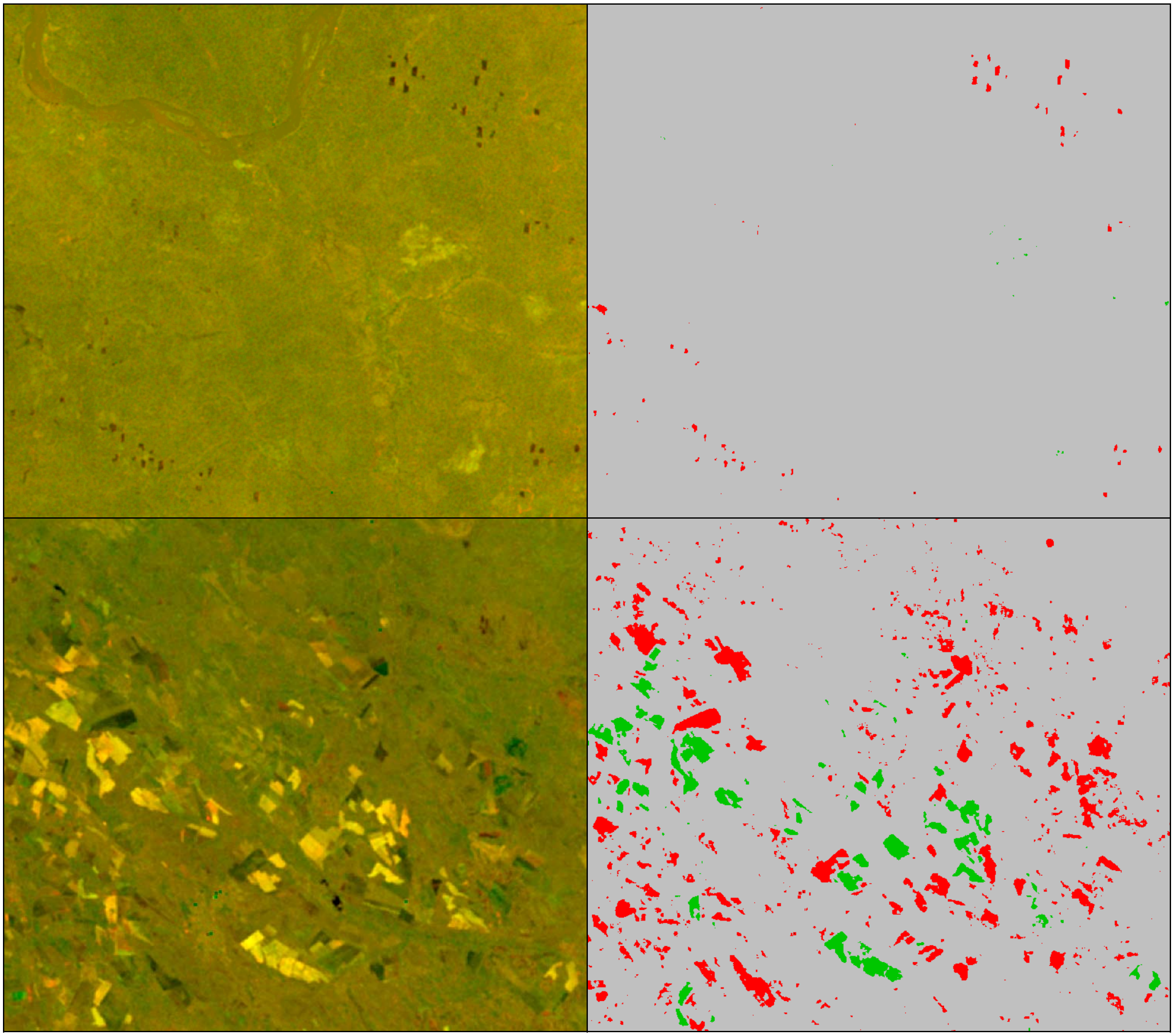

Figure 11: Input data (left column) and change map (right column). Composite and colour coding as above (Figure 9 and Figure 10). Top: forest dominated area, Bottom: agriculture dominated area**,** ALOS K&C © JAXA/METI

D. FOREST COVER MAPPING USING INTENSITY AND COHERENCE

Summer intensity and winter coherence images are used for forest monitoring. The intensities (FBD HH/HV) have been acquired during summer 2007 and feature the K&C intensity stripes. This initial investigation was carried out in the framework of GSE Forest Monitoring.

COHERENCE PROCESSING AND COMPOSITES

For the coherence estimation standard level 1.1 FBS scenes were applied. The path numbers range from 461 to 473. The 43 pairs have been acquired during the winters 2006/2007 (cycles 8 & 9) and 2007/2008 (cycles 16 & 17). Each pair stems from consecutive cycles (46 days temporal baseline). During both winters suited weather conditions (temperatures during and between acquisitions steadily far below 0°C) have been reported by representative weather stations. Interferometric processing consisted of SLC data co-registration at sub-pixel level, slope adaptive common-band filtering in range (Santoro et al. 2007), and common-band filtering in azimuth. Texture was used for the coherence computation procedure which employs an adaptive estimation approach (Wegmüller et al. 1998). All SAR images (K&C intensities and coherence) were orthorectified using SRTM elevation data. The final pixel size of the coherence is 50 by 50 m² and thus equal to the K&C data. The mosaic of the 43 coherence images is depicted in Figure 12.

A first impression of the potential of the synergistic usage of backscattering intensity and coherence can be caught from Figure 13. This RGB composite is based on the backscattering intensities HV and HH as well as the coherence. Some landcover classes can be visually separated. Water appears in black, unforested areas show up in blue, and forest covered sections appear in orange, yellow and light green colour shades. These variances are due to differing forest types and biomass levels. The light blue patch in the middle of the subset corresponds to a fire scar. Eastward from that position another small light blue patch is visible next to the water body. This one corresponds to the city of Novaja Igirma (ca. 11,000 inhabitants).

CLASSIFICATION METHODOLOGY

The presented SAR data (backscatter and coherence) provides the input for operational forest monitoring. The defined target classes as follows: forest, very low biomass forest and non-forest. Consequently, the large spectral variability of the non-forest class needs to be considered during the classification process. In fact, ten classes have been considered during the classification process. These are the classes old clear-cut, recent clear-cut, fire scar, agriculture, water, and urban plus four forest classes. For each class 20 samples have been selected under consideration of a good distribution over the whole site and accounting for the class internal variations. The class merge resulting in the three named target classes was conducted after the classification. For the classification the Nearest Neighbour algorithm was used.

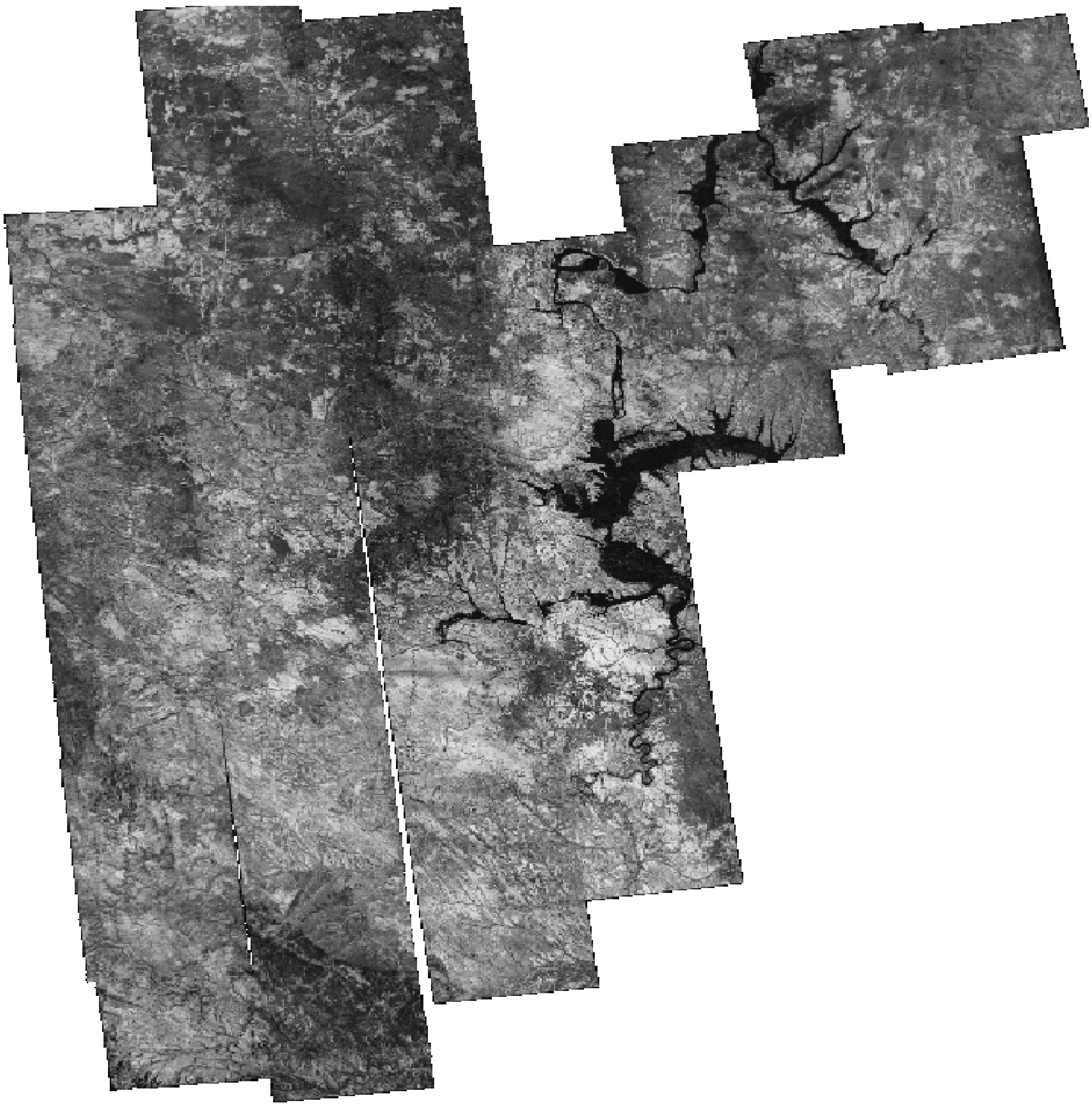

Figure 12: Mosaic of interferometric coherence images: 53°-58°N, 97°-105°E, ALOS K&C © JAXA/METI

The classification is based on image segments. The segments are identified using the multiresolution segmentation algorithm discussed by (Baatz & Schäpe 2000, Benz et al. 2004) and realised by means of the Definiens Developer software. The segments do not necessarily represent the forest compartments, but in general identify homogeneous patches. The segment size is determined by a scale parameter and can range from single pixels to the entire scene. Due to the targeted minimum mapping unit (MMU) of 1 ha, small image segments have been created. The segmentation parameter set is summarised at the following table.

Parameter	Value
Scale	2.0
Shape / Colour	0.9 / 0.1
Compactness / Smoothness	0.0 / 1.0

The segmentation process only considers the summer intensity data with the same weight of both polarisations, as the edges between the image objects are more distinct (sharp) as for the coherence. An example of a segmented image is provided in Figure 14. The provided example shows evidently, that the borders of differing adjoining patches are clearly framed. Dark blue segments represent clear cut areas which have been recently clear felled; yellow, orange and greenish sections represent different types of forest. Low biomass forest stands appear in violet shades. Although the contrast of these patches is not as strong as for the recent clear cuts, these low biomass forest stands are well captured by the segmentation.

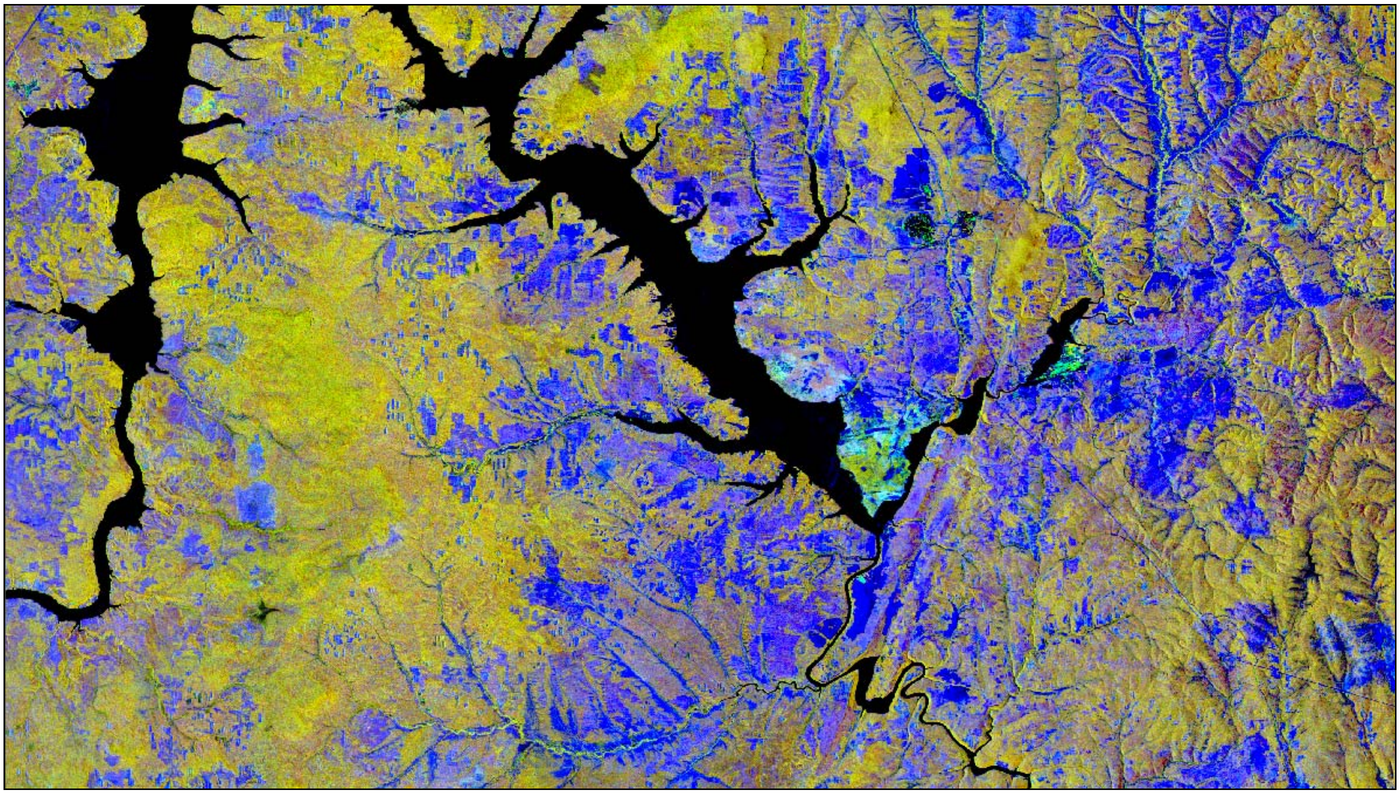

Figure 13: Composite of HV & HH backscatter and winter coherence for a subset of the monitoring area (taken from north-eastern section) , © JAXA/METI

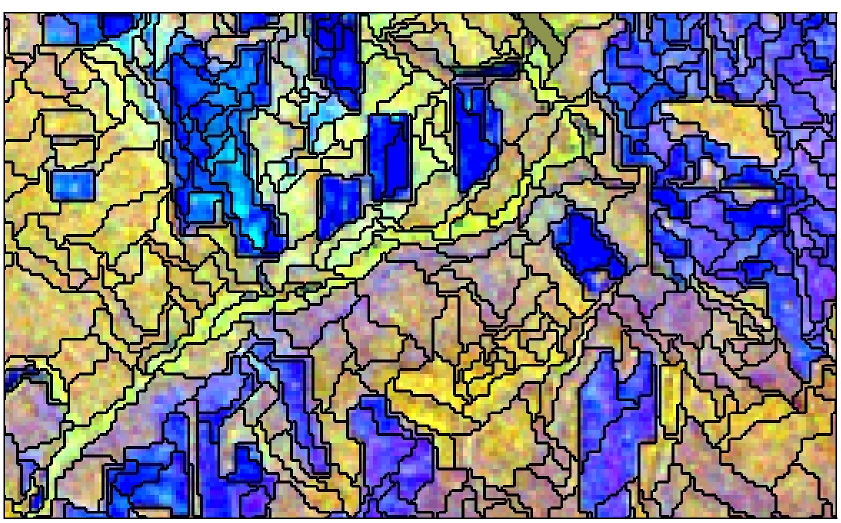

Figure 14: Example of segmented dataset, ALOS K&C © JAXA/METI

TEST AREA AND RESULTS

The test area is located in central Siberia (in the centre of the prototype area) and comprises an area of about 100,000 km² (Figure 15).

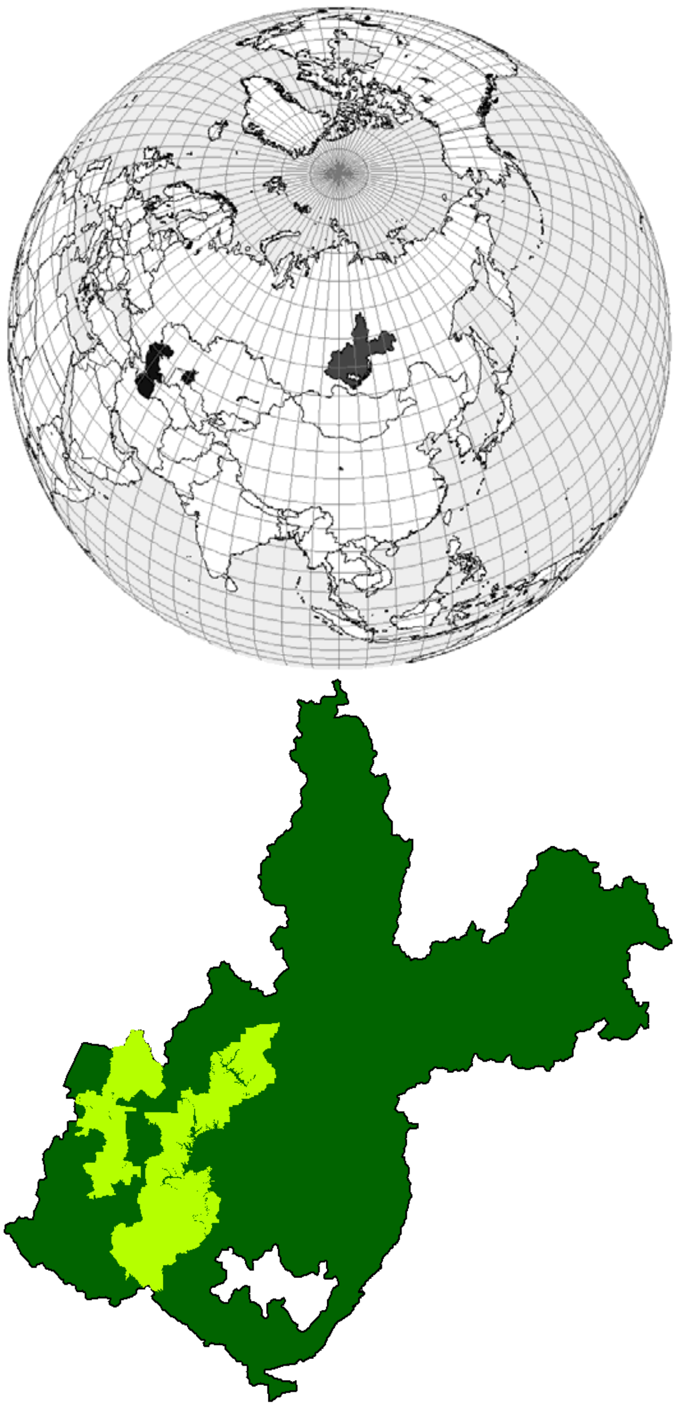

Figure 15: Test area (light green patch, right image) in the centre of the prototype area

The Middle Siberian Plateau in the southern part of the territory is characterised by hills up to 1,700 m. The northern part is flat with heights up to 500 m. Taiga forests (spruce, birch, larch, pine, etc.) dominate and cover ca. 82% of the region. The site exhibits continental climatic conditions. The yearly amount of precipitation is generally below 450 mm; the winters are very cold and dry, the summers are warm and include the precipitation season. Reference data has been available in terms of very high resolution optical data, very high resolution SAR data (TS-X), a digital forest compartment GIS data base on forest stand level, and analogue maps comprising recent and planned forest cover changes.

Figure 16 provides the SAR data and the forest cover map for the monitoring area. Figure 17 depicts a subset taken from the northern part of the provided forest cover map. The accuracy assessment for the whole monitoring area is basing on 1,000 point samples. The random sampling was stratified by class proportion. The sampling results provided the input for a standard confusion matrix. The overall accuracy of the forest cover map including the class water accounted for 90.87%. Although only three classes have been separated, an overall accuracy of 91% can be considered an excellent result. Major source of errors was some confusion between very low biomass forest and non-forest. This is due to the fact that a landscape with indiscrete landcover was separated into discrete classes. The introduction of more forest classes related to different biomass levels could overcome this handicap. However, a new potential source of confusion would be introduced. On the other hand, some confusion between diverse forest classes might be seen as awkward as between diverse land cover types. A further source of errors is the partly inexact delineation image segments. This in particular affects the classification accuracy at the edges between unlike landcover types.

Regarding the achieved map results it gets obvious, that PALSAR data are very suited for large scale forest monitoring in Siberia. In particular, the implementation of winter coherence adds a new powerful dimension to the intensity data set. Due to the well intended ALOS observation strategy coherence images can be produced for whole Siberia.

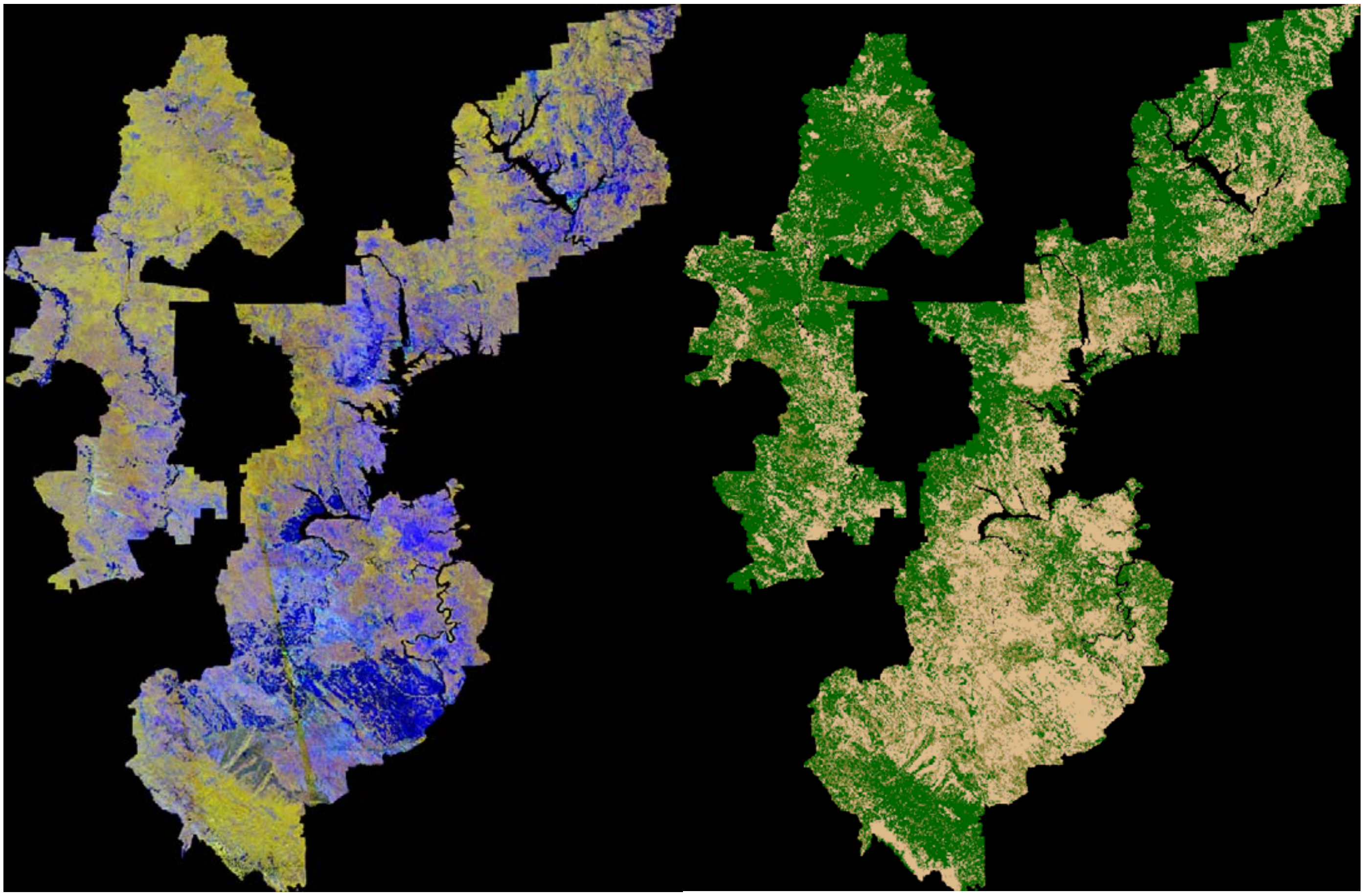

Figure 16: SAR data (left: HV/HH/Coherence) and forest cover map for the monitoring area; forest: green, very low biomass forest: brownish green, non-forest: light brown, ALOS K&C © JAXA/METI

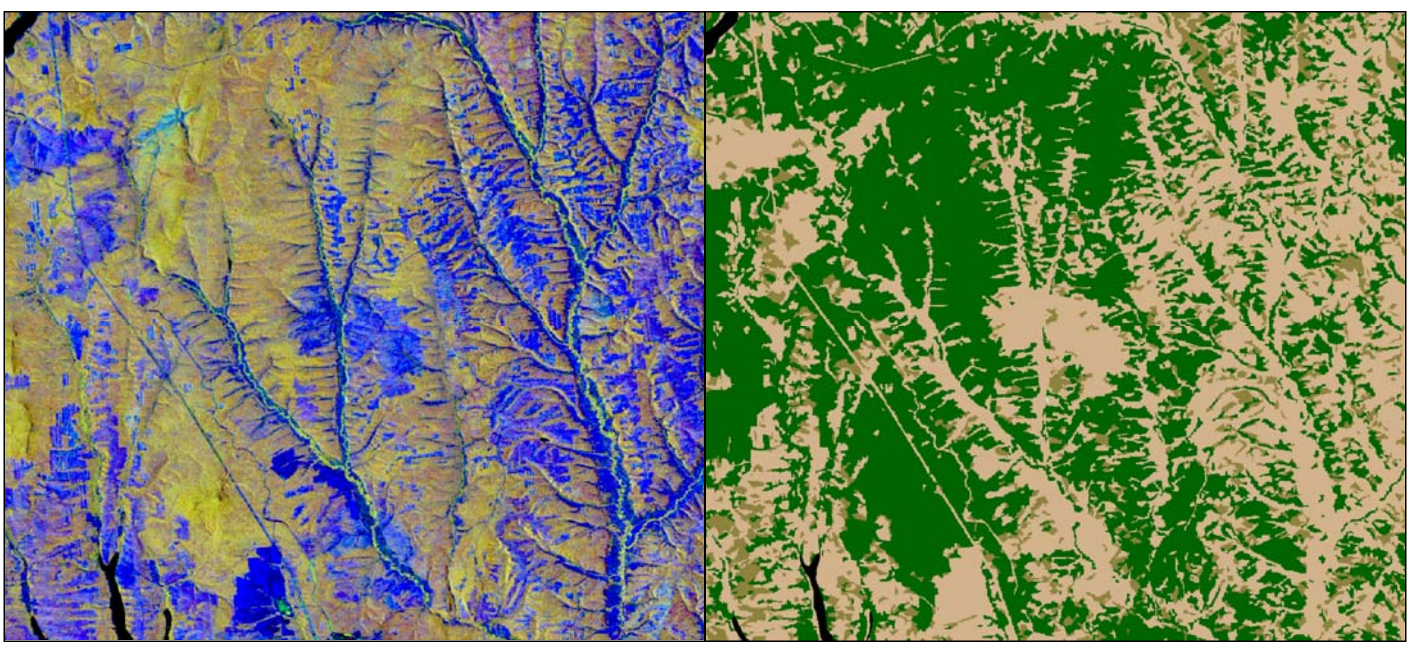

Figure 17: SAR data (HV/HH/Coherence) and forest map for subset (taken from north-eastern part) of the monitoring area; forest: green, very low biomass forest: brownish green, non-forest: light brown, ALOS K&C © JAXA/METI

4. REFERENCES

[1] Baatz, M. & A. Schäpe, “Multiresolution segmentation - an optimization approach for high quality multi-scale image segmentation” In: Strobl, J., T. Blaschke & G. Griesebner (eds) Proc. AGIT-Symposium Salzburg, Austria: 12–23, 2000.

[2] Benz, U.C., P. Hofmann, G. Willhauck, I. Langenfelder & M. Heynen, “Multi-resolution, objectoriented fuzzy analysis of remote sensing data for GIS-ready information”. ISPRS J. of Photogr. and Rem. Sens. 58: 239-258, 2004.

[3] Castel, T., A. Beaudoin, A. Stach, N. Stussi, T. LeToan & P. Durand (2001), “Sensitivity of space-born SAR data to forest parameters over sloping terrain. Theory and experiment”, Int. J. Rem. Sens. 22 (12): 2351-2376, 2001.

[4] Santoro, M., C. Werner, U. Wegmüller & O. Cartus, “Improvement of interferometric SAR coherence estimates by slope-adaptive range common band filtering”, Proc. IGARSS, Barcelona, Spain, 2007.

[5] Wegmüller, U., C. Werner, & T. Strozzi, “SAR interferometric and differential interferometric processing”, Proc. IGARSS, Seattle, USA, IEEE Publications: 1106-1108, 1998

[6] Wegmüller, U., “Automated terrain corrected SAR geo-coding”, Proc. IGARSS, Hamburg, Germany, 1999.

.

ACKNOWLEDGEMENTS

This work has been undertaken within the framework of the JAXA Kyoto & Carbon Initiative. ALOS PALSAR data have been provided by JAXA EORC.

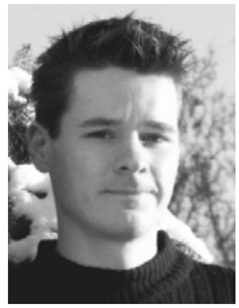

Christian J. Thiel received the Dipl. degree from the Friedrich Schiller University of Jena, Germany, in 2000 and the Ph.D. degree (with honours) from the Friedrich Schiller University of Jena, Germany, in 2004. Topic of his Ph.D. work was the investigation of polarimetric and interferometric airborne SAR data for the derivation of biophysical parameters.

Since 2004 he works as Research Project Assistant and was involved in various projects. Subject-matters have been the synergistic usage of optical and SAR-data for landcover classification, earth observation in support for transboundary aquifer management, utilisation of JERS-1 SAR-data for forest cover detection, and the operationalisation of earth observation based forestry applications. Dr. Thiel is also involved in the Kyoto and Carbon Initiative, dealing with large area PALSAR data applications focussing on forest.

Since 2006 he is chair assistant at the Earth Observation Department of the Friedrich-Schiller University Jena and head of the Radar Science and Applications section. His main scientific interests are the development and application of methods for retrieving geophysical parameters over land from active remote sensing data with a particular interest in soil moisture retrieval, forest cover mapping, and forest biomass assessment.